

# Phosphorylation of Recombinant Human ATP:Citrate Lyase by cAMP-Dependent Protein Kinase Abolishes Homotropic Allosteric Regulation of the Enzyme by Citrate and Increases the Enzyme Activity. Allosteric Activation of ATP:Citrate Lyase by Phosphorylated Sugars<sup>†</sup>

Irina A. Potapova, M. Raafat El-Maghrabi, Sergey V. Doronin, and William B. Benjamin\*

Department of Physiology and Biophysics, School of Medicine, State University of New York at Stony Brook, Stony Brook, New York 11794-8661

Received September 17, 1999; Revised Manuscript Received November 22, 1999

**ABSTRACT:** Recombinantly expressed human ATP:citrate lyase was purified from *E. coli*, and its kinetic behavior was characterized before and after phosphorylation. Cyclic AMP-dependent protein kinase catalyzed the incorporation of only 1 mol of phosphate per mole of enzyme homotetramer, and glycogen synthase kinase-3 incorporated an additional 2 mol of phosphate into the phosphorylated protein. Isoelectric focusing revealed that all of the phosphates were incorporated into only one of the four enzyme subunits. Phosphorylation resulted in a 6-fold increase in  $V_{\max}$  and the conversion of citrate dependence from sigmoidal, displaying negative cooperativity, to hyperbolic. The phosphorylated recombinant enzyme is more similar to the enzyme isolated from mammalian tissues than unphosphorylated enzyme with respect to the  $K_m$  for citrate, CoA, and ATP, and the specific activity. Fructose 6-phosphate was found to be a potent activator (60-fold) of the unphosphorylated recombinant enzyme, with half-maximal activation at 0.16 mM, which results in a decrease in the apparent  $K_m$  for citrate and ATP, as well as an increase in the  $V_{\max}$  of the reaction. Thus, human ATP:citrate lyase activity is regulated in vitro allosterically by phosphorylated sugars as well as covalently by phosphorylation.

Although hormone-directed phosphorylations of adipose and liver ATP:citrate lyase (ACL)<sup>1</sup> (EC 4.1.3.8) was first described 25 years ago (1–4), their physiological role is still not known. ACL is a homotetramer (440 kDa) that catalyzes the formation of acetyl-CoA and oxaloacetate (OAA) in the cytosol from citrate and CoA with the hydrolysis of ATP to ADP and phosphate (5). This step is a major source of cytosolic acetyl-CoA that is used in the biosynthetic pathways of fatty acids, cholesterol, and acetylcholine (6–9). This was made evident in experiments employing hydroxycitrate, a competitive ACL inhibitor which was found to severely reduce the rates of fatty acid and cholesterol biosynthesis (6). Recent findings suggest that ACL may also play an important role in gluconeogenesis, as it catalyzes the formation of a significant portion of cytosolic OAA, a major gluconeogenic precursor (10). Furthermore, ACL activity

changes, by regulating the cytosolic concentration of citrate, could modulate both glycolysis, by inhibition of phosphofructokinase (11–13), and fatty acid biosynthesis, by allosteric activation of acetyl-CoA carboxylase (ACC) (14).

Rat ACL gene expression and protein content are increased at the transcriptional level by caloric intake and insulin, and are decreased by starvation and in diabetes mellitus (9, 15). The in vivo phosphorylation of mammalian ACL also changes in response to nutrients and the hormonal milieu in cultured hepatocytes and during the differentiation of 3T3-L1 cells into adipocytes (16).

Three regulatory phosphorylation sites in ACL have been identified (17) that are distinct from the catalytic autophosphorylation site (His 760), an intermediate in the catalysis of the enzyme (18, 19). These are Thr 446 and Ser 450, which are phosphorylated by glycogen synthase kinase-3 (GSK-3) (17, 20), and Ser 454, which is phosphorylated by the catalytic subunit of cAMP-dependent protein kinase (PKA) (21, 22) or by an “insulin-stimulated kinase(s)” (23–27). These three phosphorylation sites comprise a peptide motif that is homologous to similar domains in other proteins, including glycogen synthase (17), that are phosphorylated by GSK-3 (28). Rat liver ACL phosphorylations also exhibit site–site interactions (28–30), and the phosphorylation of a first PKA targeted site carboxyl to the others is a prerequisite for phosphorylations catalyzed by GSK-3.

The overall phosphorylation state of ACL varies widely depending on the hormonal challenge. For example, insulin decreases ACL phosphorylation at Thr 446 and Ser 450 (16,

<sup>†</sup> This work was supported by New York State Research Council Bridge Grant CO 14149.

\* To whom correspondence should be addressed at the Department of Physiology and Biophysics, School of Medicine, State University of New York at Stony Brook, Stony Brook, NY 11794-8661. Tel.: 516-444-3046; FAX: 516-444-3432; E-mail: wbenjamin@physiology.pnb.sunysb.edu.

<sup>1</sup> Abbreviations: ACC, acetyl-CoA carboxylase; ACL, ATP:citrate lyase; CoA, coenzyme A; DTT, dithiothreitol; ECL, enhanced chemiluminescence; Fru 6-P, fructose 6-phosphate; Glu 6-P, glucose 6-phosphate; GSK-3, glycogen synthase kinase-3; hACL, human ACL; IEF, isoelectric focusing; IPTG, isopropyl-1-thio- $\beta$ -D-galactopyranoside; OAA, oxaloacetate; PKA, catalytic subunit of cAMP-dependent protein kinase; PMSF, phenylmethylsulfonyl fluoride; rACL, rat ACL; SDS–PAGE, sodium dodecyl sulfate–polyacrylamide gel electrophoresis.

17) by inhibiting GSK-3 activity (31) and/or by activation of a phosphatase (32), whereas it increases the phosphorylation of Ser 454 catalyzed by an "insulin-stimulated kinase". This site is also phosphorylated in response to glucagon or  $\beta$ -adrenergic receptor agonists, via the activation of PKA (24, 33).

Despite these changes in ACL phosphorylation due to hormonal or dietary manipulations, it had not been possible to show any significant concomitant alteration in ACL activity as a function of these challenges, when enzyme was assayed in cell lysates (33, 34) or in preparations purified from tissues (33, 35). Covalent regulation of ACL activity was consequently dismissed as being insignificant in the regulation of fatty acid or cholesterol synthesis. This notion was reinforced by the fact that ACL, as isolated from mammalian tissues, or expressed in insect or Chinese hamster ovary cells, is already phosphorylated to varying degrees, before or during isolation (36, 37), as well as the enzyme's known susceptibility to proteolysis (5), all of which contribute to the ambiguities prevalent in the literature regarding ACL regulation. It thus became apparent that to clearly define the covalent regulation of ACL activity, it would be necessary to purify an enzyme form free of posttranslational modifications. Because eukaryotic enzymes expressed in *E. coli* are known to be relatively free of such processing, we have used this system to express the human and rat ACL in a catalytically active unphosphorylated form, and to kinetically characterize the effects of phosphorylation, and of allosteric effectors. We report herein that hACL is phosphorylated in vitro on only one of its four subunits, and that its activity is increased both by phosphorylation and by phosphorylated sugars.

## MATERIALS AND METHODS

**Materials.** Full-length human and rat liver cDNAs of ACL in pBluescript were a gift of Dr. M. O. Elshourbagy, SmithKline Beecham Pharmaceuticals. The pET3a and pET15b expression vectors and host *E. coli* strains, BL21(DE3) and BL21(DE3)pLysS, were obtained from Novagen. A plasmid encoding the bacterial chaperonins GroES and GroEL (pREP4-GroESL) was a kind gift of Dr. M. Stieger, Hoffmann-La Roche, Basel, Switzerland. Rabbit polyclonal antibodies against purified rat ACL holoenzyme, for immunoprecipitation and Western blotting studies, were obtained as previously described (16). GSK-3 was purified as previously described (20, 38). CoA, ATP, NADH, D-fructose 6-phosphate, D-glucose 6-phosphate, D-fructose 2,6-diphosphate, D-fructose 1,6-diphosphate, D-xylulose 5-phosphate, D-glucose 1-phosphate, D-ribulose 5-phosphate, 6-phosphogluconic acid, D-ribose 5-phosphate, D-erythrose 4-phosphate, DL-glyceraldehyde 3-phosphate, phospho(enol)pyruvate, glycerol 2-phosphate, glycerol 3-phosphate, DL-1-glycerophosphate, uridine 5'-diphosphoglucose, D-(+)-glucose, L-glucose, N-acetyl-D-glucosamine, L- $\alpha$ -phosphatidylinositol, D-myoinositol 4,5-bisphosphate, D-myoinositol 1,4,5-trisphosphate, D-myoinositol 1,3,4,5-tetrakisphosphate, malic dehydrogenase, and PKA were from Sigma. [ $\gamma$ - $^{32}$ P]ATP (10 mCi/mL), ECL kit, and Western blotting reagents were from Amersham. Ampicillin, IPTG, and DTT were from U. S. Biochemical Corp. Acrylamide, as a 40% solution, bisacrylamide, as a 2% solution, T4 DNA ligase, and calf intestinal alkaline phosphatase (molecular biology grade)

were from Boehringer Mannheim Corp. SDS-PAGE molecular weight standards, high range (regular or prestained), and Kaleidoscope prestained markers were from Bio-Rad. Sephacryl S-200, Sepharose CL-4B, and Immobiline Dry-Plates (pH 4–7), broad pI kit, and reagents were from Pharmacia Biotech. Restriction enzymes, Taq Track sequencing kit, and dNTP were obtained from New England Biolabs. All other reagents and solvents were of reagent grade.

**Methods.** Oligonucleotides complementary to the 5'- and 3'-untranslated sequences of the ACL cDNA were synthesized on an Applied Biosystems 381A DNA synthesizer. Amplification was carried out in a Corbett fast thermal sequencer using a thermocycler programmed for 35 cycles of denaturation (30 s at 94 °C), annealing (30 s at 55 °C), and extension (3 min at 72 °C). *E. coli* strains were grown in LB media (pH 7.5) at 37 or 25 °C for approximately 6 h to  $A_{600} = 1.0$ . The antibiotics used for colony selection were as follows: ampicillin, 100  $\mu$ g/mL for all strains; and chloramphenicol, 17  $\mu$ g/mL for pLysS-containing strains, and/or kanamycin, 30  $\mu$ g/mL for pGroESL-containing strains. For the protein inductions, a single colony was used to inoculate LB medium containing the appropriate antibiotic(s), and cultures were shaken for about 8 h at 25 °C until  $A_{600}$  reached between 0.5 and 1.0. The medium was made 25 mM glucose and 0.5% v/v glycerol, the induction of ACL was initiated by the addition of IPTG to the medium to a final concentration of 1 mM, and growth was continued for 24 h. Aliquots were removed at different times of the induction, and bacterial proteins were analyzed by SDS-PAGE.

Human cDNA was amplified from full coding length hACL cDNA by PCR using synthetic oligonucleotide primers complementary to the immediate 5'- and 3'-sequences of the cDNA and encoding unique restriction sites. The 5'-primers coded an *Nde*I restriction site and the hACL initiation codon, and were complementary to the -13+13 region of the sequence. The 3'-primer encoded a *Hind*III restriction site, complementary to bases 3342–3387 of the hACL sequence (36, 37), and also modified the 3'-untranslated sequence to eliminate a naturally occurring *Nde*I site. The resulting product (3.4 kb) was purified by electrophoresis in 1% agarose gels, digested with *Nde*I and *Hind*III, and ligated into the similarly digested T7 RNA polymerase-based expression plasmid pET3a, and the product was used to transform competent *E. coli* (71/18 strain). Thus, the entire translated sequence of human ACL was subcloned in pET3a downstream of the  $\phi$ 10 promoter which is highly specific for T7 RNA polymerase (39), and was designated as hACL.pET3a. The plasmid DNA was isolated and purified, and both strands were sequenced by automated DNA sequencing and were identical to hACL-2 (36, 37), suggesting that no changes were introduced by PCR.

Rat liver ACL was subcloned using the same strategy, by amplifying the coding sequence of rACL cDNA using PCR with two oligonucleotide primers: one encoding an *Nde*I restriction site and the translation initiation, and the other encoding an *Eco*RI restriction site. The resulting plasmid was designated as rACL.pET3a. We have also subcloned the hACL and rACL sequences into a pET15b vector, which encodes ACL as a fusion protein with six amino-terminal histidyl residues.

The protein concentration of the soluble cell lysate was measured by the Bradford Bio-Rad Protein Assay using bovine serum albumin as a standard. The amount of hACL in the purified enzyme fraction was estimated from the Coomassie Blue staining intensity of the ACL subunit after SDS-PAGE, using bovine serum albumin as a standard, and the protein concentration of the sample. ACL activity was measured in the bacterial extracts using the malic dehydrogenase coupled assay. For the extract preparation, bacteria were harvested by centrifugation at 5000g for 10 min and resuspended in 50 mM Tris-HCl buffer, pH 8.0, containing 1 mM EDTA, 100 mM NaCl, 0.5 mM 2-mercaptoethanol, 25% glycerol, 2  $\mu$ g/mL aprotinin, 1  $\mu$ g/mL pepstatin A, 100  $\mu$ g/mL PMSF, and 1 mg/mL lysozyme. The cells were disrupted by three cycles of freezing and thawing, and the cell debris was removed by centrifugation. Standard molecular biological techniques were used for all these procedures. Plasmid DNA was purified by CsCl isopycnic ultracentrifugation (40), and sequencing was done with dideoxy chain termination (41) using Taq DyeDeoxy Terminator kits from ABI and the appropriate vector or internal primers. Routine analytical procedures, including SDS-PAGE and Western blotting, were performed as described (16, 42). Isoelectric focusing studies (IEF) were performed as described in the protocols supplied by Pharmacia Biotech.

**Phosphorylation Studies.** Phosphorylated hACL forms were prepared by incubating the enzyme at 30 °C in 50 mM Tris-HCl (pH 8.0), 0.5 mM EDTA, 5 mM MgCl<sub>2</sub>, 4 mM DTT, and 0.5–2 mM ATP (0.1 mM when using [ $\gamma$ -<sup>32</sup>P]ATP with specific activity 1250 cpm/pmol) with PKA or GSK-3 or with both kinases. Freeze-dried PKA that had been reconstituted at 4 °C with water containing DTT (50  $\mu$ g/ $\mu$ L) and glycerol [final concentration 35% (v/v)] was stored at –20 °C. ACL concentration in the phosphorylation mixture was 40  $\mu$ g/mL. To measure phosphorylation, samples were preincubated for 5 min at 25 °C in the phosphorylation reaction mixture without ATP. Reactions were initiated by the addition of [ $\gamma$ -<sup>32</sup>P]ATP. Samples were removed (10  $\mu$ L) at different time intervals, and the reaction was terminated by the addition of “sample buffer”, so that the final concentration contained 0.1% SDS, 10 mM Tris-HCl (pH 7.5), 10 mM 2-mercaptoethanol, 10% (v/v) glycerol, and 0.002% Bromphenol blue. Samples were boiled for 5 min. ACL was resolved from other proteins by SDS-PAGE on 7.5% polyacrylamide gels. The gels were stained with Coomassie brilliant blue, and the protein content of the ACL band was estimated as described. After destaining in 7.5% acetic acid, gels were either dried or exposed wet (wrapped in “Saran Wrap”) to X-ray films overnight. Washing the gels in acetic acid removed all catalytic phosphate, so that incubations with [ $\gamma$ -<sup>32</sup>P]ATP but without PKA showed no radioactivity associated with the ACL subunit. For quantification, the ACL subunit was excised and placed in a vial containing scintillation fluid for radioactivity measurement by scintillation spectroscopy. For calculation purposes, the subunit molecular mass was 120 kDa. For kinetic analysis after phosphorylation, samples were cooled on ice, glycerol was added to 35% concentration, and they were stored at –20 °C until use.

**Assay of Enzyme Activity.** ACL activity was assayed by the coupled malic dehydrogenase method (5, 42). One unit of activity equals 1  $\mu$ mol of NADH oxidized/min at 37 °C. The

standard assay mixture consisted of 50 mM Tris-HCl (pH 8.0), 10 mM MgCl<sub>2</sub>, 1.9 mM DTT, 0.15 mM NADH, 0.07 mM CoA, 1 mM ATP, 2 mM potassium citrate, and 3.3 units/mL malic dehydrogenase. Assays were conducted at 25 or 37 °C in a temperature-controlled Beckman recording kinetic spectrophotometer.

**Kinetic Studies.** All kinetic experiments were carried out at 37 °C by varying one substrate concentration while keeping the concentrations of the other constituents constant and at more than 5 times their  $K_m$  values. All constants were calculated by Sigma Plot (Version 4.01) statistical analysis function. The apparent  $V_{max}$  and  $K_m$  values for citrate (for both PKA and PKA- and GSK-3-phosphorylated forms of hACL), CoA, and ATP were calculated by computer fitting the initial data to the hyperbolic form of the Michaelis–Menten equation by a double reciprocal plot of  $1/v$  versus  $1/S$ . In experiments to determine citrate  $K_m$ , CoA and ATP were maintained constant at 0.07 and 1 mM, respectively, and citrate concentrations were varied from 0.05 to 5.0 mM. For ATP  $K_m$  determinations, CoA and citrate were maintained constant at 0.07 and 2 mM, and ATP concentrations were varied from 0.125 to 2 mM. In CoA  $K_m$  determinations, citrate and ATP were held constant at 2 and 1 mM, respectively, and CoA concentrations were varied from 4 to 40  $\mu$ M.  $S_{0.5}$ ,  $A_{0.5}$ , and the Hill coefficient values for substrates and allosteric activators were determined by analyzing the data according to a transformation of the Hill equation:  $\log(v/V_{max} - v) = n_H \log S - \log K$ , where  $v$  is the ACL catalytic rate,  $n_H$  is the Hill coefficient constant,  $S$  is the concentration of citrate, and  $K$  is a constant. Under these conditions, the constant ( $K$ ) is  $S_{0.5}$  and approximates the  $K_m$  value predicted by the Michaelis–Menten equation.  $V_{max}$  for the Hill equation was estimated by  $v$  versus  $v/S$  plot. All experiments were repeated 3–5 times, and the standard error in the determinations of  $K_m$ ,  $S_{0.5}$ , Hill coefficient, and  $V_{max}$  values did not exceed 20% between independent assays.

## RESULTS

**Expression of hACL and rACL.** Four *E. coli* strains were transformed with hACL.pET3a or hACL.pET15b plasmids to optimize the recombinant expression: (1) BL21(DE3), a  $\lambda$  lysogen carrying a single genomic copy of the T7 RNA polymerase gene under the control of the inducible lacUV5 promoter; (2) BL21(DE3)pLysS carrying pLysS, a pET-compatible plasmid that produces T7 lysozyme, thereby reducing the basal level of target gene transcription; and (3) BL21(DE3)pGroESL or (4) BL21(DE3)pLysS/pGroESL, each containing a plasmid that coexpresses the two bacterial chaperonins GroES and GroEL, which have been reported to increase the folding, solubility, and biological activity of eukaryotic proteins expressed in *E. coli* (43).

As shown in Figure 1, expression of hACL in the four bacterial strains showed that the highest yield of ACL protein was obtained using the BL21(DE3)pGroESL strain. Our initial attempts to purify N-His<sup>6</sup>-tagged ACL on nickel columns were unsuccessful, even though the His-tag appeared to have no effect on either the yield or the kinetics of ACL (data not shown). We then substituted pET3a for the His-tag encoding vector pET15b and carried out all of the studies reported in this paper on nonfusion ACL purified by conventional means.



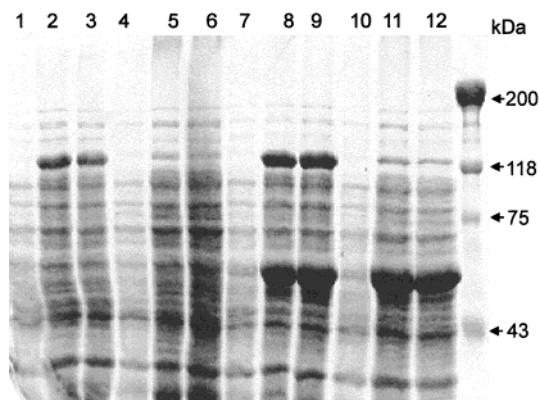


FIGURE 1: Expression of hACL in four strains of *E. coli*. Bacterial cells transfected with N-His<sup>6</sup>-hACL.pET15b were lysed at 0 h (lanes 1, 4, 7, 10), 18 h (lanes 2, 5, 8, 11), and 24 h (lanes 3, 6, 9, 12) after addition of IPTG. Lysate proteins were resolved by SDS-PAGE, and the gel was stained with Coomassie Brilliant Blue R250. Lanes 1–3, 4–6, 7–9, and 10–12 contain protein from BL21-(DE3), BL21(DE3)pLysS, BL21(DE3)pGroESL, and BL21(DE3)-pGroESL.pLysS *E. coli* strains, respectively. The migrations of molecular mass markers are as indicated.

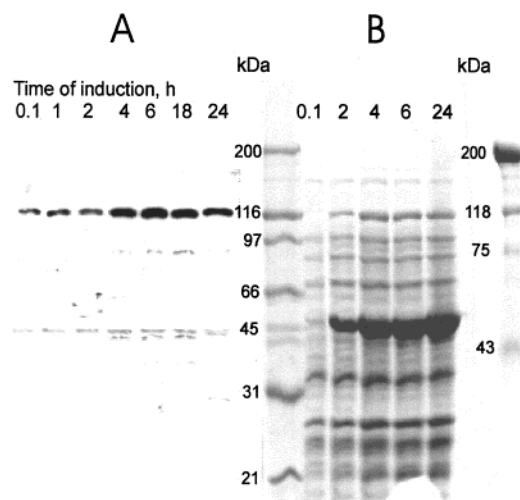


FIGURE 2: Immunoreactivity of hACL expressed in BL21(DE3)-pGroESL *E. coli*. Bacterial cells were transfected with hACL.pET3a. Cells were lysed at various time intervals after the addition of IPTG. Proteins in the lysate were resolved on duplicate SDS-PAGE. One set of samples was transferred to nitrocellulose, and after incubation with anti-ACL antibodies, the enzyme subunit was visualized by Western blotting by enhanced chemiluminescence (panel A). The other gel was stained with Coomassie Brilliant Blue R250 (panel B). The times elapsed after induction by IPTG and the migration of molecular mass markers are as indicated.

To confirm that the expressed protein was immunologically the ACL subunit, cells were harvested at different time points, and protein was resolved in duplicate on polyacrylamide gels (Figure 2), one of which was transferred to nitrocellulose for Western blots. A single band of immunoreactive ACL subunit was detected in the induced bacteria that was minimally visible in uninduced bacteria, but was absent in cells carrying vectors only (data not shown). An immunoreactive band(s), in low abundance, was (were) noted at the region of the gel in which the chaperonin Gro EL migrates. This immunoreactivity may represent a spurious antibody binding to Gro EL or to a proteolytic product of, or partially synthesized ACL.

The apparent molecular weight of the induced band corresponded approximately to 120 000, the expected value for the hACL subunit, consistent with a deduced  $M_r$  of 121 419 of the 1105 amino acid sequence (15, 36, 37). This value is also in good agreement with the apparent  $M_r$  of approximately 120 000 on SDS-PAGE for the ACL subunit purified from mammalian tissues (3, 4).

Based on activity measurements, the yield of soluble and enzymatically active ACL protein was estimated to be about 20 mg/L, with little or no ACL activity detected in extracts from bacteria transformed with vector alone. The expression of both rACL and hACL at room temperature was detected as early as 2 h after induction, and the recombinant protein continued to accumulate for at least 24 h, with 18 h of induction being optimal for the highest amount of enzymatically active recombinant hACL. With longer induction times, a larger fraction of ACL was recovered in the insoluble fraction, and there was greater proteolysis of the protein.

**Purification of hACL.** Bacterial cell extracts from BL21-(DE3)pGroESL containing the hACL.pET3a plasmid were fractionated by ammonium sulfate precipitation, and the hACL was purified by gel filtration and anion exchange chromatography (DE 52). The inclusion of 10% glycerol and 2–10 mM citrate in all buffers during purification and storage greatly increased the recovery and stability of ACL as shown in ref 44. Bacteria were harvested by centrifugation, washed 3 times with 10 mM potassium phosphate (pH 7.5), containing 0.1 mM EDTA and 10 mM NaCl, and stored as a frozen “wet cell pellet” (approximately 3 g of packed cells per liter of culture). All subsequent steps were carried out at 4 °C. Packed cells were suspended in approximately 5 volumes of lysis buffer A [10 mM potassium phosphate (pH 7.5), 5 mM potassium citrate, 0.2 mM EDTA, 15 mM 2-mercaptoethanol, 10% glycerol, 0.2 mM PMSF, and 1  $\mu$ g/mL each of pepstatin, aprotinin, and leupeptin] and lysed by sonication on ice with 10, 30 s bursts alternating with 30 s of cooling. The lysate was clarified by centrifugation. Saturated ammonium sulfate was added to the supernatant to a 15% final saturation, and the resulting precipitate was removed by centrifugation. The supernatant was then adjusted to 40% saturation with ammonium sulfate, and the precipitated ACL was collected by centrifugation for 1 h at 28000g. The pellet was dissolved in a minimal volume of buffer A, and the sample was loaded onto a Sephacryl S200 gel filtration column (50 cm  $\times$  1.5 cm) equilibrated with buffer A. The column was eluted with 120 mL of buffer A, and the fractions containing the peak of activity were pooled.

The sample was then applied to a DE 52 anion exchange column (50 cm  $\times$  2 cm), equilibrated with buffer A, containing 10 mM potassium citrate and 5 times the concentration of all protease inhibitors (buffer B). The column was washed with several volumes (800 mL) of equilibration buffer until the  $A_{280}$  approached that of the buffer alone. Protein was eluted from the column with an 800 mL linear gradient of 10–200 mM phosphate in buffer B. ACL eluted at about 50 mM phosphate, and fractions containing enzyme activity were pooled. The enzyme preparation was concentrated about 5-fold, by ultrafiltration on Biomax-100K NMWL membranes (Amicon), to a final protein concentration of 0.2 mg/mL, glycerol was added to 35% (v/v) concentration, and the preparations were stored

Table 1: Purification of Human ATP:Citrate Lyase Expressed in *E. coli*<sup>a</sup>

step	volume (mL)	protein (mg)	activity (units)	sp act. (units/mg)	purification (x-fold)	yield (%)
cell-free extract	27	1262	105	0.083	1	100
15–45% (NH <sub>4</sub> ) <sub>2</sub> SO <sub>4</sub> precipitate	9.1	876	73.6 <sup>b</sup>	0.084 <sup>b</sup>	1 <sup>b</sup>	60.6
Sepharose 4B-200	45	105	21.9	0.209	2.5	20.9
DE 52	9.1	1.9	3.8	2.0	24.1	3.6

<sup>a</sup> Human liver ATP:citrate lyase was expressed in 2 L of LB media. The expressed protein was purified and assayed as described under Methods. <sup>b</sup> These values are underestimated as NH<sub>4</sub> ion inhibits ACL activity.

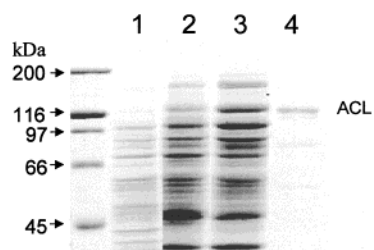


FIGURE 3: Purification of hACL expressed in *E. coli* cells. Proteins at each step of purification were resolved by SDS–PAGE and stained with Coomassie Brilliant Blue R250. Lane 1, lysate soluble proteins from BL21(DE3)pGro cells prior to IPTG induction, 10  $\mu$ g; lane 2, lysate proteins after IPTG induction, 50  $\mu$ g; lane 3, proteins after gel exclusion chromatography, 50  $\mu$ g; lane 4, proteins after DE 52 chromatography, 1  $\mu$ g. Molecular mass standards are as indicated.

at  $-20^{\circ}\text{C}$ . The specific activity of the final preparation was typically 2.0 units/mg at  $37^{\circ}\text{C}$ .

Aliquots from the various steps of the purification were assayed for enzyme activity and analyzed by SDS–PAGE (Table 1 and Figure 3). Using this purification scheme, about 2 mg of an approximately 80% pure preparation of hACL could be obtained from 2 L of bacterial culture (Table 1). Recombinant enzyme differed from that purified from mammalian tissues in not showing any evidence of proteolysis on SDS–PAGE after storage at  $-20^{\circ}\text{C}$  for 1 year or after incubation at  $30^{\circ}\text{C}$  for 4 h. The minor lower molecular weight bands, noted on SDS–PAGE, were not consistent with their being proteolytic cleavage products, as they were not immunoreactive on Western blots and not radioactive when the holoenzyme was first phosphorylated by PKA and GSK-3 using  $[\gamma\text{-}^{32}\text{P}]\text{ATP}$  as phosphoryl donor. The relative amounts of these protein bands compared to the major hACL band did not increase during storage or incubation of hACL as described above.

To further characterize hACL, the protein was studied by gel exclusion chromatography on Sepharose 4B. Human ACL was eluted on gel filtration in the same relative fractions as was bovine thyroglobulin (669 kDa). This result is in accord with findings using hACL cloned in baculovirus-infected insect cells (37), and ACL from oleaginous yeast (45) and green sulfur bacterium (46), as these findings also demonstrated that the enzyme eluted with thyroglobulin. As ACL has been determined to be approximately 480 kDa in sedimentation velocity experiments (5), and approximately

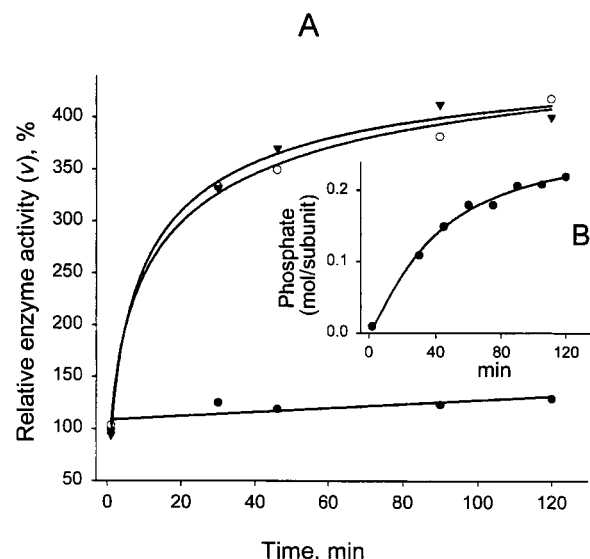


FIGURE 4: Effect of phosphorylation on hACL activity. Panel A: hACL was incubated as described under Methods with 1.0 mM ATP but without kinase (●), with PKA (○), or with PKA and GSK-3 (▼). Enzyme activity was measured at various time intervals as described under Methods. The final concentrations of citrate, CoA, and ATP in these assays were 2, 0.07, and 1 mM, respectively. Inset panel B: Phosphate incorporated into hACL, by PKA and 0.1 mM  $[\gamma\text{-}^{32}\text{P}]\text{ATP}$ . At various time intervals, 20  $\mu\text{L}$  aliquots from the reaction mixture were mixed with 5  $\mu\text{L}$  of 5 $\times$  SDS sample buffer and heated at  $100^{\circ}\text{C}$  for 5 min, and the mixture was subjected to SDS–PAGE. The radioactive hACL band was cut from the gel, and phosphate incorporation was measured.

120 kDa on SDS–PAGE, and taking into account its cDNA amino acid sequence (36, 37), it is suggested that the 480 kDa holoenzyme assumes an eccentric shape in solution.

**Phosphorylation of hACL.** Unlike previous reports concerning ACL expressed in insect or Chinese hamster ovary cells (36, 37), hACL as isolated from *E. coli* appears to be unphosphorylated. The incorporation of phosphate into hACL protein catalyzed by PKA, with respect to time and its effect on ACL activity, is shown in Figure 4. In 10 separate experiments there was a significant and rapid increase in enzyme activity that broadly correlated with its phosphorylation reaching a maximum when 0.25 mol of phosphate was incorporated per subunit or up to 1 mol/mol of holoenzyme. This value is lower than that found previously (2–4 mol/mol of holoenzyme), using enzyme purified from fat or liver (5, 28, 34–36). This level of phosphorylation was not increased by varying the concentrations of the reaction components, by increasing the ratio of catalytic subunit to hACL, or by increasing the time of incubation to 24 h, or after 2 h of incubation by adding extra PKA and ATP followed by another 2 h of incubation (data not shown). These results are consistent with experiments that also showed that the incorporation of phosphate into glycogen synthase often does not correspond stoichiometrically with the number of sites expected to be phosphorylated (28, 29).

As previously reported (28, 47), unphosphorylated hACL was not a substrate for phosphorylation by GSK-3 added alone. However, when hACL was first phosphorylated by PKA to its maximum level (0.25 mol of phosphate per subunit), and then phosphorylated by the addition of GSK-3, an additional 0.5 mol of phosphate per subunit could be

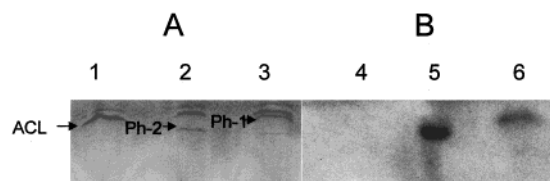


FIGURE 5: Isoelectric focusing of the unphosphorylated, PKA, and PKA- and GSK-3-phosphorylated forms of hACL. After phosphorylation of hACL by PKA or by PKA and GSK-3, samples were prepared for IEF as described. Lanes 1 and 4, unphosphorylated hACL incubated without protein kinase; lanes 2 and 5, hACL phosphorylated with PKA and GSK-3; lanes 3 and 6, hACL phosphorylated with PKA. Panel A: Proteins were resolved by IEF in denaturing and reducing conditions as described in the *Pharmacia Biotech Bulletin* and stained with Coomassie Brilliant Blue R250 (lanes 1–3). The samples were allowed to enter the gel by electrophoresis at 1.5 kV for 1 h. The samples were resolved by electrophoresis at 5.0 kV for 4 h. Panel B: Autoradiography of the stained gel (lanes 4–6). The positions of the hACL-unphosphorylated subunit (approximate isoelectric pH of 8.65), the phosphorylated subunit that most likely contains three phosphate groups (Ph-2, approximate isoelectric pH of 8.15), and the subunit that most likely contains one phosphate group (Ph-1, approximate isoelectric pH of 8.4) are shown on the Coomassie-stained gel. A broad *pI* kit (*pI* range 3.5–9.3) was used to estimate the isoelectric points of these polypeptides. The radioactive band in lanes 5 or 6 was associated with Ph-2 (lane 2) or Ph-1 (lane 3), respectively.

incorporated. These results are consistent with the total incorporation of 0.75 mol of phosphate per mole of subunit.

Because the results presented above are suggestive of single-site reactivity, i.e., only one of the subunits being phosphorylated, the various phosphorylated ACL species were subjected to isoelectric focusing. Using Immobiline plates (pH 4–7) and a urea/DTT/Triton X-100 mixture, unphosphorylated ACL was focused near pH 8.65 (Figure 5A, lane 1) as two bands, the major band focused at this more acidic pH, and represented about 80% of the total protein as estimated by densitometric measurements of the Coomassie blue stained gel. The other, more basic-focusing band was present in all three samples and could be a contaminant or an oxidation product of ACL. It is not likely to be the holoenzyme as this protein should be too large to migrate on this gel. ACL that had been phosphorylated by PKA focused as three distinct bands (Figure 5A, lane 3), one of which contained all of the incorporated radioactivity (4491 arbitrary units) and it focused at about pH 8.4 (Figure 5B, lane 6). This band was estimated by densitometric measurements to be about one-fourth of the total ACL. The other two bands did not contain any radioactivity, focusing at the same pHs as those of unphosphorylated hACL. A possible explanation for the focusing behavior is that only one of the four subunits is phosphorylated, presumably on Ser 454. ACL that had been phosphorylated by both PKA and GSK-3 also focused as three distinct bands (Figure 5A, lane 2), two of which, about three-fourths of the total protein, focused at the same pH as the unphosphorylated enzyme and were not radioactive. The third band, containing all of the radioactivity (Figure 5B, lane 5), focused at an even more acidic pH than any other form (pH 8.15), and constituted about one-fourth of the mass of the total protein. Densitometric analysis of the autoradiograph showed about 2.7 times more radioactivity (12 075 arbitrary units) than that incorporated into the hACL subunit phosphorylated by PKA alone. These data are consistent with the hypothesis that only one

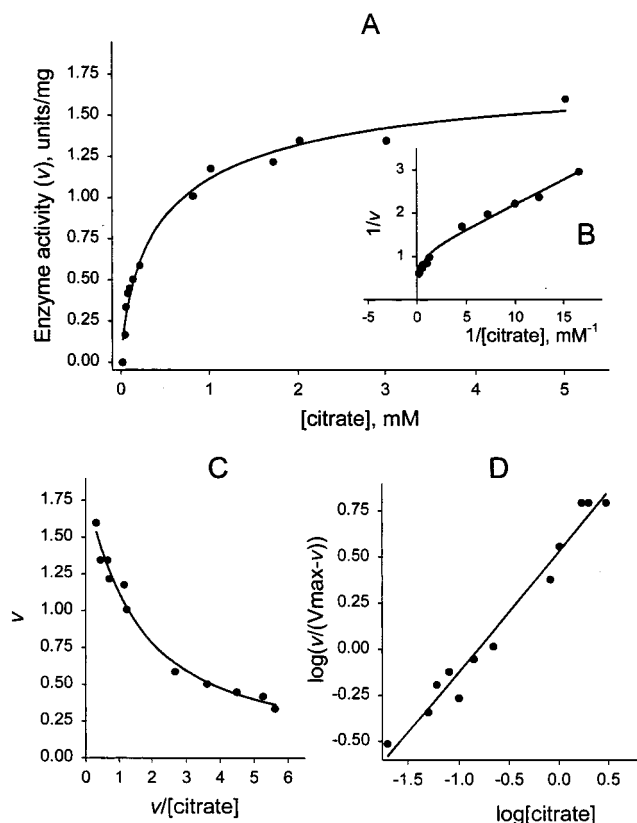


FIGURE 6: Activity of unphosphorylated hACL as a function of citrate concentration. Assays were conducted as described under Methods in a total volume of 750  $\mu$ L. Reaction was initiated by the addition of unphosphorylated hACL. Panel A: Velocity plot. The steady-state rate of citrate cleavage normalized to enzyme concentration was measured by varying the citrate concentration for fixed saturating concentrations of ATP and CoA. Curves are the best fit obtained by nonlinear regression analysis of the experimental data to the sigmoidal equation. Plots B, C, and D are derived from the data in panel A. Panel B: Lineweaver–Burk plot. Panel C: Eadie–Hofstee plot. The curves are the best fits obtained by nonlinear regression analysis of the data. Panel D: Hill plot of the citrate binding curve of hACL. The  $V_{max}$  value for the Hill plot was estimated from panel C. The degree of cooperative binding of citrate to hACL and the  $S_{0.5}$  for citrate were determined by analyzing the data according to a transformation of the Hill equation.

of the four subunits is accessible to phosphorylation by GSK-3, one that had been phosphorylated previously by PKA.

**Effect of Phosphorylation on hACL Kinetic Properties.** Maximal hACL activity increased 3-fold with incorporation of phosphate into the enzyme (Figure 4). In fact, phosphorylation by PKA alone appeared to be sufficient to fully activate ACL, suggesting that subsequent phosphorylation of the enzyme by GSK-3 might affect other enzyme parameters.

The dependence of unphosphorylated hACL activity on one substrate (citrate) is shown in Figure 6 and Table 2. At lower substrate concentrations, the dependence appears to follow Michaelis–Menten kinetics, but displays negative cooperativity at higher citrate concentrations. This is more evident when the data are analyzed either as double reciprocal plots (Figure 6B) or as an Eadie–Hofstee plot ( $v$  versus  $v/S$ ) (Figure 6C). A Hill plot of the citrate dependence gives a coefficient of binding of 0.65 (Figure 6D), reflecting weak negative cooperativity. This cooperative behavior is abolished



Table 2: Steady-State Kinetic Parameters<sup>a</sup> for the Unphosphorylated and Phosphorylated Forms of Human ATP:Citrate Lyase Expressed in *E. coli*

Fru 6-P (1 mM)	hACL form					
	unphosphorylated		PKA-phosphorylated		PKA/GSK-3-phosphorylated	
	—	+	—	+	—	+
$V_{\max}$ (units/mg) for citrate	—	—	10.1 <sup>b</sup>	—	10.5 <sup>b</sup>	—
$K_m^b$ for citrate <sup>d</sup> ( $\mu$ M)	1.8 <sup>c</sup>	16.3 <sup>c</sup>	10.2 <sup>c</sup>	25.2 <sup>c</sup>	10.6 <sup>c</sup>	25.5 <sup>c</sup>
$S_{0.5}^e$ ( $\mu$ M)	154	8	103	45	115	30
Hill coefficient <sup>e</sup> for citrate	0.65	0.49	0.91	0.58	0.99	0.62
$K_m$ for CoA <sup>d,f</sup> ( $\mu$ M)	2.59	2.32	2.01	2.35	2.28	2.09
$K_m$ for ATP <sup>d</sup> ( $\mu$ M)	41.00	2.89	41.15	4.79	37.8	4.01
$V_{\max}^b$ (units/mg) for ATP	3.1	9.7	11.0	12.3	12.8	12.0

<sup>a</sup> The data shown are from one representative set of experiments. <sup>b</sup> Calculated using the Lineweaver–Burk equation. <sup>c</sup> Calculated using the Eadie–Hofstee equation. <sup>d</sup> All other substrates were at saturating concentrations (3.5 mM, 70  $\mu$ M, and 1 mM for citrate, CoA, and ATP, respectively). <sup>e</sup> Calculated using the Hill equation. <sup>f</sup> Assayed at 8 mM Glu 6-P, without 1 mM Fru 6-P.

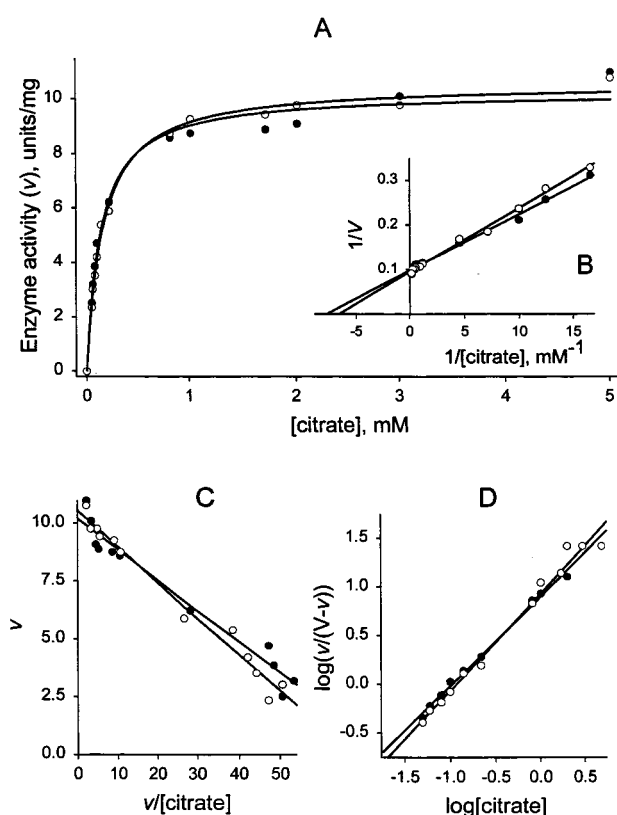


FIGURE 7: Activity of the phosphorylated forms of hACL as a function of citrate concentration. Assays were conducted and data were analyzed as described in Figure 7. PKA-phosphorylated (●); PKA- and GSK-3-phosphorylated (○). Panel A: Velocity plots. The curves are the best fit by nonlinear regression analysis of the experimental data to a hyperbolic equation. Panel B: Lineweaver–Burk plots used for the determination of the kinetic constants ( $K_m$  and  $V_{\max}$ ). Panel C: Eadie–Hofstee plots. Panel D: Hill plots of citrate binding to the two phosphorylated forms of hACL.  $V_{\max}$  values for the corresponding Hill plots were estimated from the equations used in panels B and C.

when the enzyme is phosphorylated either by PKA alone or in combination with GSK-3 (Figure 7).

In this series of experiments, in addition to the greater than 6-fold increase in specific activity with phosphorylation, citrate dependence reverted to Michaelis–Menten distribution throughout the curve (Figure 7B,C). No difference

between ACL phosphorylated by PKA or by PKA and GSK-3 was again noted, and both had Hill coefficient values close to 1.0 (Figure 7D and Table 2). There was no significant difference in the  $K_m$  for citrate between unphosphorylated ACL and either of the phosphorylated forms of ACL (Table 2). Similarly, there was no difference in the Michaelis–Menten constants for CoA and ATP between the unphosphorylated ACL and both phosphorylated forms of hACL (Table 2). The apparent CoA  $K_m$ , calculated from the Lineweaver–Burk plots, was 2.59  $\mu$ M for unphosphorylated ACL, 2.01  $\mu$ M for PKA-phosphorylated ACL, and 2.28  $\mu$ M for PKA- and GSK-3-phosphorylated ACL, whereas that for ATP was 41.0  $\mu$ M, 41.15  $\mu$ M, and 37.8  $\mu$ M for each form, respectively.

**ACL Activation by Phosphorylated Sugars.** The phosphorylation state of the site 3 domain of glycogen synthase, which is a target for phosphorylation by GSK-3 (17), determines the enzyme's sensitivity to Glu 6-P. Because there is a homologous region to site 3 of glycogen synthase in the phosphorylation domain of hACL, it was of importance to test the effects of various sugar phosphates on ACL activity, and to determine whether its enzyme kinetic values in the presence of sugar phosphates were altered by phosphorylation. We had previously shown that rat liver ACL is activated at 2–4 mM Glu 6-P (48). However, the extent of activation and the reproducibility of these observations varied with the preparation and storage of the enzyme (unpublished results). Unphosphorylated hACL was found to be consistently activated by Glu 6-P, with a  $K_a$  in the 2–5 mM range (data not shown). The effect of Glu 6-P was to increase the maximal rate of catalysis, up to 27-fold, with no change in the affinities for any of the substrates (data not shown). PKA and PKA- and GSK-3-phosphorylated hACL were also activated by millimolar amounts of Glu 6-P but to a lesser extent (data not shown).

Other sugar phosphates, structurally similar to Glu 6-P, were also tested to determine if they affected ACL enzyme kinetics (Table 3). Among those examined, in addition to Glu 6-P, Fru 6-P, fructose 2,6-bisphosphate, ribulose 5-phosphate, and fructose 1,6-bisphosphate were found to be activators of hACL. Fru 6-P was the most potent activator, causing approximately a 60-fold increase in the maximal activity of unphosphorylated hACL, at concentrations that

Table 3: Effect of Different Phosphorylated Sugars and Their Analogues on the Activity of Unphosphorylated hACL<sup>a</sup>

substances	activation <sup>b</sup>	substances	activation <sup>b</sup>
D-fructose 6-phosphate	38.5 ± 1.9 <sup>c</sup> (55.4 ± 0.6)	phospho(enol)-pyruvate	1.3 ± 0.2
D-glucose 6-phosphate	26.6 ± 1.3 (5.2 ± 0.1)	glycerol 2-phosphate	1.0 ± 0.1
D-fructose 2,6-diphosphate	13.7 ± 2.0 (4.1 ± 0.5)	DL-α-glycero-phosphate	1.0 ± 0.1
D-fructose 1,6-diphosphate	3.8 ± 0.7 (1.2 ± 0.2)	uridine 5'-diphosphoglucose	1.1 ± 0.1
D-glucose 1-phosphate	1.7 ± 0.3	D-(+)-glucose	1.1 ± 0.1
D-ribulose 5-phosphate	5.5 ± 0.6 (1.2 ± 0.1)	L-glucose	1.0 ± 0.1
D-xylulose 5-phosphate	1.3 ± 0.1	N-acetyl-D-glucosamine	1.0 ± 0.1
6-phosphogluconic acid	1.2 ± 0.1	L-α-phosphatidylinositol	1.0 ± 0.1 <sup>d</sup>
D-ribose 5-phosphate	1.1 ± 0.1	D-myoinositol 4,5-bisphosphate <sup>b</sup>	0.9 ± 0.1 <sup>d</sup>
D-erythrose 4-phosphate	1.0 ± 0.1	D-myoinositol 1,4,5-trisphosphate <sup>b</sup>	0.9 ± 0.1 <sup>d</sup>
DL-glyceraldehyde 3-phosphate	1.0 ± 0.1	D-myoinositol 1,3,4,5-tetrakisphosphate <sup>b</sup>	1.1 ± 0.1 <sup>d</sup>

<sup>a</sup> All substrates at 3.5 mM, 70 μM, and 1 mM for citrate, CoA, and ATP, respectively. <sup>b</sup> Activation is times activated at either 10 or 1 (in parentheses) mM. <sup>c</sup> Mean ± range, *n* = 3. <sup>d</sup> Activation at 0.01 mM.

were an order of magnitude less than those needed for Glu 6-P activation (Figure 8 and Table 2). A 30-fold activation was seen at 0.1 mM Fru 6-P, which is well within the physiological range for this sugar phosphate in liver (49), whereas maximal activation was observed at approximately 1 mM Fru 6-P (Figure 8, Tables 2 and 3). The concentration of fructose 1,6-bisphosphate required for half-maximal ACL activation, or apparent  $K_a$ , was intermediate between, Glu 6-P and Fru 6-P. The calculated  $K_a$  values were  $0.16 \pm 0.09$ ,  $3.34 \pm 0.32$ , and  $0.56 \pm 0.50$ , for Fru 6-P, Glu 6-P, and fructose 1,6-bisphosphate, respectively (Table 3). The linearity of the Lineweaver–Burk plots for Fru 6-P dependence is consistent with noncooperative binding to the enzyme (Figure 8). Similar results were found for Glu 6-P (data not shown).

The binding of Fru 6-P affected almost all of the kinetic properties of unphosphorylated hACL. In addition to increasing the  $V_{\max}$  of the reaction, it caused a greater than 90% reduction in the  $K_m$  values for ATP and citrate, with little or no effect on the  $K_m$  for CoA (Table 2). Enzyme that was phosphorylated by PKA or by PKA and GSK-3 was less sensitive to activation by sugar monophosphates, with  $V_{\max}$  values increasing only 2–3 times, compared to 10–20 times for unphosphorylated ACL (Table 3).

## DISCUSSION

ATP:citrate lyase catalyzes a reaction that is central to three important biochemical pathways: fatty acid and cholesterol biosynthesis, and gluconeogenesis, by virtue of the nature of its two products, acetyl-CoA and oxaloacetate. The regulation of its activity can, therefore, be considered appropriate for fuel transport and storage as well as replenishment. However, rapid regulation of ACL's activity by changes in caloric intake and hormones has not been shown.

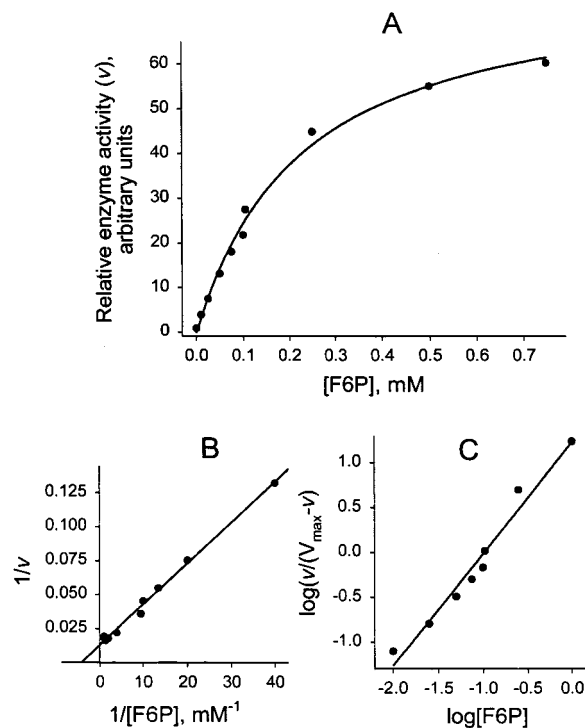


FIGURE 8: Dependence of the relative activity of unphosphorylated hACL on [Fru 6-P]. Panel A: Velocity plots. The steady-state rate of citrate cleavage normalized to the initial velocity without added Fru 6-P was measured at various Fru 6-P concentrations at fixed saturating concentrations of citrate, ATP, and CoA as described under Methods. Reaction was initiated by addition of enzyme. The curve is the best fit obtained by nonlinear regression analysis of the experimental data to the sigmoidal equation. Panel B: Lineweaver–Burk plot used for the determination of  $A_{0.5}$ . Panel C: Hill plot of Fru 6-P binding to the nonphosphorylated hACL. The  $V_{\max}$  value for the Hill plot was estimated from the equation used in panel B.

An essential requirement for the proper kinetic analysis of enzymes is the maintenance of primary as well as higher orders of structure of the purified enzyme. ACL has been purified from a variety of tissues, as well as expression systems, and a common denominator has been highly variable kinetic and regulatory properties. Enzyme isolated from eukaryotic tissues is highly susceptible to proteolysis (5) as well as posttranslational modifications, which are probably some of the reasons for the widely diverging specific activities reported: 0.8–21 units/mg of protein (3–5, 36, 37, 50–53). Furthermore, in vitro phosphorylation of the enzyme has also been highly variable in outcome and has failed to significantly change enzyme kinetic parameters; all of these observations have reinforced the conclusion that there is no rapid regulation of ACL's activity and that the phosphorylation of this enzyme is inconsequential.

The bacterial recombinant system used in this study relies on the lack of posttranslational processing of eukaryotic proteins expressed in protease-deficient bacteria. Three encouraging factors contribute to the reliability of these recombinant ACL preparations: a consistent specific activity, about 2.0 units/mg of protein (37 °C); the lack of any apparent proteolytic products; and the reproducibility of PKA- and GSK-3-dependent phosphorylations. Phosphorylation of these preparations catalyzed by PKA was found to increase the maximal activity of the enzyme by approximately 3–6-fold. These observations suggest a reason for



the inconsistent specific activities previously reported, namely, variable degrees of phosphorylations, either in the cell or during isolation, producing an enzyme with variable specific activities. The kinetic parameters of *in vitro* phosphorylated hACL were found to be similar to those of ACL purified from mammalian tissues or those expressed in eukaryotic cells (36, 37), which is consistent with the above explanation.

Since all the data appear to indicate the phosphorylation of only one of the four subunits, we conclude that the enzyme displays single-site reactivity with respect to phosphorylation; i.e., the phosphorylation of one subunit has an inhibitory effect on the phosphorylation of the other three subunits. One possible explanation for the increased level of phosphorylation of ACL isolated from mammalian tissues could be a partial unfolding or proteolysis of the enzyme that abolished the single-site reactivity and/or exposed heretofore "unavailable" phosphorylation sites (5).

The dependence of GSK-3-catalyzed phosphorylation on PKA-phosphorylated hACL, which is consistent with previous results, using enzyme from mammalian tissues (28, 38, 47), suggests a hierarchical order, similar to that described for glycogen synthase, cAMP-dependent protein kinase R II subunit, inhibitor-2 of type 1 phosphatase, G-subunit of type 1 phosphatase, hormone-sensitive lipase, and ACC (28). All of the changes in ACL's kinetic parameters were observed with the initial PKA-catalyzed phosphorylation, with no further detectable changes with the subsequent GSK-3-catalyzed phosphorylations. It is possible, however, that GSK-3-catalyzed phosphorylation of ACL could have an effect on enzyme stability, intracellular targeting, or protein–protein interactions leading to specific phosphatase or protease activity. Studies are in progress to determine the thermal stability and phosphatase or trypsin sensitivity of PKA- and GSK-3-phosphorylated hACL compared to the unphosphorylated form.

During refeeding, ACL constitutes approximately 3–5% of the total cytosolic protein in rodent liver and adipose tissues (33, 54). Studies by Avruch (33, 54), that measured ACL phosphorylation levels *in vivo*, found that after hormone stimulation the level of phosphorylation approached 0.2 mol of phosphate per subunit. Based on this finding, and the fact that ACL activity *in vitro* was not altered with phosphorylation, they suggested that ACL phosphorylation was "incidental". As a significant proportion of ACL in adipocytes is apparently in the unphosphorylated form (16) and our study found that the *in vitro* phosphorylation of hACL by PKA is also only 0.25 phosphate per subunit, it is likely that the previous *in vivo* studies (33) accurately measured physiological levels of phosphorylation. However, their conclusion that phosphorylation had no physiological effect should be reexamined in light of the studies reported in this paper.

The marked activation of ACL upon phosphorylation by PKA is consistent with the proposed physiological consequences. Increased hepatic intracellular cAMP and the associated activation of PKA are characteristics of increased hepatic gluconeogenesis. ACL activation by PKA-dependent phosphorylation, and the resulting increased production of the gluconeogenic substrate OAA, is consistent with the changes in metabolism (14, 55). Other kinetic consequences of ACL phosphorylation are more difficult to explain. For example, unphosphorylated hACL was found to behave as

a homotropic allosteric enzyme with respect to citrate, displaying negative cooperativity at higher citrate concentrations (Figure 6). In some enzyme preparations, non-Michaelis–Menten dependence of the rate of citrate cleavage on citrate concentration had been observed previously but not studied (35, 56–58). This behavior, in our preparations, is abolished by PKA-catalyzed phosphorylation (Figure 7). The physiological significance of negative cooperativity for the unphosphorylated enzyme in the cell (Figures 6 and 7) could be the maintenance of a constant ACL activity throughout a wide range of citrate concentrations. Phosphorylation of the enzyme, by eliminating the negative cooperativity with respect to citrate, would convert ACL into a form that is even more active at lower citrate levels, and its increased activity would tend to inhibit a rise in citrate concentration, which might be inappropriate during catabolism.

Because the allosteric regulation by citrate primarily affects the rate of the enzymatic reaction, the enzyme is classified as a  $V_{\max}$  type homotropic allosteric enzyme (59), and is consistent with the finding that a maximum of only 2 mol of phosphate is incorporated at the catalytic histidyl residue per enzyme tetramer (60). According to the negative cooperativity model (61), binding of the first ligand molecule to one of the four potential catalytic sites decreases the affinity of the other sites on the enzyme for ligand. In the noncooperative form, it is proposed that all citrate binding sites are equivalent and noninteractive. Changes in the allosteric properties of oligomeric enzymes, resulting from the modification of a single amino acid, have been reported (62). It is not known whether the catalytic (His 760) and regulatory sites (phosphorylation sites or Fru 6-P binding domain) are all on the same or different subunits of the holoenzyme.

In addition to control of hACL activity by phosphorylation, it was found that the enzyme's activity is also regulated by phosphorylated sugars. Fru 6-P, at near-physiological concentrations (50–100  $\mu$ M) (49), increases the activity of unphosphorylated hACL (Figure 8). The maximal activity of unphosphorylated hACL was increased approximately 20-fold by 0.1 mM Fru 6-P, and approximately 50-fold by 0.5 mM Fru 6-P (Figure 8). Although the  $V_{\max}$  of the phosphorylated enzyme was also increased, the extent of activation by Fru 6-P was less than that of the unphosphorylated form (data not shown). Comparison of the effects of a variety of phosphorylated and nonphosphorylated sugars on the activation of hACL suggests that the phosphate group at the 6-position and the orientation of the hexose backbone are required for optimal interaction. For example, the addition of an additional phosphate at the 1-position of Fru 6-P (Fru 1,6-P<sub>2</sub>) or the substitution of glucose for fructose (Glu 6-P) increases the apparent  $K_a$  by 4- and 20-fold, respectively. Other kinetic parameters were also affected by Fru 6-P; the apparent  $K_m$  values for citrate and ATP, but not CoA, were reduced by approximately 85% (Table 2), suggesting that Fru 6-P induces a conformational change in the binding site for this substrate. The latter are components of the first rate-limiting stage of the ACL-catalyzed reaction, in which His-760 is phosphorylated by ATP, followed by the transfer of phosphate to citrate to form citryl phosphate within the active site (15, 19). GSK-3-targeted phosphorylations do not influence the interaction of hACL with Fru 6-P. In light of these new findings, the allosteric role of sugar monophosphates on ACL activity can, therefore, be considered a

positive feedback mechanism to ensure the maintenance of increased gluconeogenic flux, because one of the primary means of glucagon action to increase gluconeogenic flux is to increase hepatic Fru 6-P at the expense of Fru 1,6-P<sub>2</sub>.

It is proposed that the regulation of ACL activity by phosphorylation and allostery can, at least in part, explain the effects of glucagon to increase gluconeogenic flux by increasing OAA availability. Rosiers et al. (10) concluded that in the starved rat the ACL pathway would account for the transfer of 40% of the OAA carbon atoms used for glucose synthesis that came from lactate. On the other hand, ACL is catalytically active in livers from both fed and fasted animals (10), an observation that has led to the long-held belief that it is a "house-keeping" enzyme whose regulation is insignificant. Alternatively, it can be argued that ACL is part of two seemingly opposing biosynthetic pathways: gluconeogenesis and fatty acid biosynthesis, both essential to meet the needs of the organism, and that phosphorylation of ACL in both metabolic states can account for its activation. In the fasting state, glucagon acts via PKA to phosphorylate and activate ACL, whereas in the fed state, insulin acts via "an insulin-stimulated kinase" to phosphorylate, most likely the same Ser-454, and activate ACL. This formulation is consistent with previous results (20) which showed that insulin action in vivo decreases the phosphorylation of the GSK-3-targeted sites but increases the phosphorylation of Ser 454, the target of PKA and other protein kinases (24, 63). One possible candidate for an "insulin-stimulated protein kinase" is Akt (PKB). The minimum sequence motif required for efficient phosphorylation by Akt has been determined to be Arg-X-Arg-Y-Z-Ser/Thr-Hyd, where X is any amino acid, Y any small residue other than glycine, and Hyd is phenylalanine or leucine (64). In the ACL-phosphorylatable sequence, Ser 454 is three residues carboxyl to Arg 451 and one residue amino terminal to phenylalanine 455, making Ser 454 a possible Akt target site.

In the fasted state, with the fuel supply from the catabolism of fatty acids, gluconeogenesis and also mitochondrial and cytosolic citrate levels are increased (65–68). At the same time, due to its phosphorylation by PKA, ACL is activated and is now noncooperative. These changes boost the supply of OAA, the substrate for glucose production in the cytosol, and could lower citrate concentration. Fatty acid synthesis is suppressed by inhibition of ACC activity due to its phosphorylation and possibly by a relative decrease in citrate concentration (69). Gluconeogenesis is activated by a rise in acetyl-CoA levels, a potent activator of pyruvate carboxylase, as it is no longer being consumed by fatty acid synthesis, a consequence of inhibition of ACC activity. Allosteric regulation of ACL by Fru 6-P, which activates and increases its negative cooperativity, would play a modulatory role in determining the metabolic fate of the substrate and products of ACL catalysis.

In view of the results presented in this paper, the complexity of ACL activity regulation, albeit a non-rate-limiting enzyme, which involves both phosphorylation and allostery, seems almost inevitable as both substrate (citrate) and products (acetyl-CoA and OAA) are allosteric regulators of other enzymes that control vital metabolic pathways or act as substrates for these controlled pathways. Small changes in the rates of enzymes at the beginning of a biochemical pathway may produce significant changes in the rate of

production of the end product of a pathway composed of many enzymes (70). Work is in progress to express dominant negative and positive mutants of ACL in cultured cells, in which the phosphorylation site(s) has (have) been either abolished or mimicked, to determine the contribution of each to the hormonal regulation of intermediary metabolism.

## ACKNOWLEDGMENT

We thank Dr. M. O. Elshourbagy, SmithKline Beecham Pharmaceuticals, for the gift of human and rat liver full-length cDNAs of ACL and Dr. Todd Miller of our department for his helpful discussion. The assistance of the Health Research Council of the State of New York is especially appreciated.

## REFERENCES

1. Benjamin, W. B., and Singer, I. (1974) *Biochim. Biophys. Acta* 251, 28–42.
2. Benjamin, W. B., and Singer, I. (1975) *Biochemistry* 14, 3301–3309.
3. Ramakrishna, S., and Benjamin, W. B. (1979) *J. Biol. Chem.* 254, 9232–9236.
4. Alexander, M. C., Kowaloff, E. M., Witters, L. A., Dennihy, D. T., and Avruch, J. (1979) *J. Biol. Chem.* 254, 8052–8056.
5. Linn, T. C., and Srere, P. A. (1979) *J. Biol. Chem.* 254, 1691–1698.
6. Sullivan, A. C., Triscari, J., Hamilton, J. C., Miller, O., and Wheatley, V. R. (1973) *Lipids* 9, 121–128.
7. Gribble, A. D., Dolle, R. E., Shaw, A., McNair, D., Novelli, R., Novelli, C. E., Slingsby, B. P., Shah, V. P., Tew, D., Saxty, B. A., Allen, M., Groot, P. H., Pearce, N., and Yates, J. (1996) *J. Med. Chem.* 39, 3569–3584.
8. Patel, M. S., and Owen, O. E. (1976) *Biochem. J.* 156, 603–607.
9. Towle, H. C., Kaytor, E. N., and Shih, H.-M. (1997) *Annu. Rev. Nutr.* 17, 405–433.
10. Rosiers, C. D., Donato, L. D., Comte, B., Laplante, A., Marcoux, C., David, F., Fernandex, C. A., and Brunengraber, H. (1995) *J. Biol. Chem.* 270, 10027–10033.
11. Garland, P. B., Randle, P. J., and Newsholme, E. A. (1963) *Nature* 200, 169–170.
12. Barron, J. T., Kopp, S. J., Tow, J., and Parillo, J. E. (1994) *Am. J. Physiol.* 267, H764–H769.
13. Comte, B., Vincent, G., Bouchard, B., and Rosiers, C. D. (1997) *J. Biol. Chem.* 272, 26117–26124.
14. Reilly, D. I., and Allred, J. B. (1997) *Prog. Lipid Res.* 35, 371–385.
15. Elshourbagy, N. A., Near, J. C., Kmeysz, P. J., Sathe, G. M., Southan, C., Strickler, J. E., Gross, M., Young, J. F., Wells, T. N. C., and Groot, P. H. E. (1990) *J. Biol. Chem.* 265, 1430–1435.
16. Benjamin, W. B., Pentyala, S. N., Woodgett, J. R., Hod, Y., and Marshak, D. (1994) *Biochem. J.* 300, 477–482.
17. Ramakrishna, S., D'Angelo, G., and Benjamin, W. B. (1990) *Biochemistry* 29, 7617–7624.
18. Houston, B., and Nimmo, H. G. (1984) *Biochem. J.* 224, 437–443.
19. Wells, T. N. C. (1991) *Eur. J. Biochem.* 199, 163–168.
20. Hughes, K., Ramakrishna, S., Benjamin, W. B., and Woodgett, J. R. (1992) *Biochem. J.* 288, 309–314.
21. Pierce, M. W., Palmer, J. L., Keutmann, H. T., Hall, T. A., and Avruch, J. (1981) *J. Biol. Chem.* 256, 8867–8870.
22. Pierce, M. W., Palmer, J. L., Keutmann, H. T., Hall, T. A., and Avruch, J. (1982) *J. Biol. Chem.* 257, 10681–10686.
23. Price, D. J., Nemenoff, R. A., and Avruch, J. (1989) *J. Biol. Chem.* 264, 13825–13833.
24. Yu, K. T., Benjamin, W. B., Ramakrishna, S., Khalaf, N., and Czech, M. P. (1990) *Biochem. J.* 265, 539–545.
25. Young, W., Tavare, M., and Proud, C. G. (1994) *Biochem. J.* 303, 15–20.

26. Holman, G. D., and Kasuga, M. (1997) *Diabetologia* 40, 991–1003.
27. Shepherd, P. R., Nave, B. T., and Middle, K. (1995) *Biochem. J.* 305, 25–28.
28. Roach, P. J. (1991) *J. Biol. Chem.* 266, 14139–14142.
29. DePaoli-Roach, A. A., Ahamad, Z., Camici, M., Lawrence, J. C., Jr., and Roach, P. J. (1983) *J. Biol. Chem.* 258, 10702–10709.
30. Ramakrishna, S., Pucci, D. L., and Benjamin, W. B. (1983) *J. Biol. Chem.* 258, 4950–4956.
31. Ramakrishna, S., and Benjamin, W. B. (1988) *J. Biol. Chem.* 263, 12677–12681.
32. Wera, S., and Hemmings, B. A. (1995) *Biochem. J.* 311, 17–29.
33. Avruch, J., Nemenoff, R. A., Pierce, M., Kwok, Y. C., and Blackshear, P. J. (1985) *Molecular Basis of Insulin Action* (Czech, M. P., Ed.) pp 263–296, Plenum Press, New York.
34. Ranganathan, N. S., Srere, P. A., and Linn, T. C. (1980) *Arch. Biochem. Biophys.* 204, 52–58.
35. Pentylala, S. N., and Benjamin, W. B. (1995) *Biochemistry* 34, 10961–10969.
36. Elshourbagy, N. A., Near, J. C., Kmetz, P. J., Wells, T. N. C., Groot, P. H. E., Saxty, B. A., Hughes, S. A., Franklin, M., and Gloger, I. S. (1992) *Eur. J. Biochem.* 204, 491–499.
37. Lord, K. A., Wang, X.-M., Simmons, S. J., Bruckner, B. C., Loscig, J., O'Connor, B., Bentley, R., Smallwood, A., Chadwick, C. C., Stevis, P. E., and Ciccarelli, R. B. (1997) *Protein Expression Purif.* 9, 133–141.
38. Ramakrishna, S., and Benjamin, W. B. (1985) *J. Biol. Chem.* 260, 12280–12286.
39. Studier, F. W., and Moffat, B. A. (1986) *J. Mol. Biol.* 189, 113–130.
40. Sanger, F., Nicklen, S., and Coulson, R. R. (1977) *Proc. Natl. Acad. Sci. U.S.A.* 74, 5463–5467.
41. Sambrook, J., Fritsch, E. F., and Maniatis, T. (1989) *Molecular Cloning: A Laboratory Manual*, 2nd ed., Cold Spring Harbor Laboratory, Cold Spring Harbor, NY.
42. Takeda, Y., Suzuki, F., and Inoue, H. (1967) *Methods in Enzymology* (Lowenstein, J. M., Ed.) Vol. 13, pp 153–160, Academic Press, New York.
43. Amrein, K. E., Takacs, B., Stieger, M., Molnos, J., Flint, N. A., and Burn, P. (1995) *Proc. Natl. Acad. Sci. U.S.A.* 92, 1048–1052.
44. Vogel, H. J., and Bridger, W. A. (1981) *J. Biol. Chem.* 256, 11702–11707.
45. Shashi, K., Bachhawat, A. K., and Joseph, R. (1990) *Biochim. Biophys. Acta* 1033, 23–30.
46. Wahlund, T. M., and Tabita, F. R. (1997) *J. Bacteriol.* 170, 4859–4867.
47. Ramakrishna, S., Murthy, K. S., and Benjamin, W. B. (1989) *Biochemistry* 28, 856–860.
48. Benjamin, W. B., and Pentylala, S. N. (1995) Abstract 200, ASBMB National Meeting.
49. Cottam, G. L., and Srere, P. A. (1969) *Biochem. Biophys. Res. Commun.* 35, 859–900.
50. Szutowicz, A., and Srere, P. A. (1983) *Arch. Biochem. Biophys.* 221, 168–174.
51. Houston, B., and Nimmo, H. G. (1984) *Biochem. J.* 224, 437–443.
52. Wraight, C., Day, A., Googenraad, N., and Scopes, R. (1985) *J. Biol. Chem.* 260, 604–609.
53. Houston, B., and Nimmo, H. G. (1985) *Biochim. Biophys. Acta* 844, 233–239.
54. Alexander, M. C., Palmer, J. C., Pointer, R. H., Koumjian, L., and Avruch, J. (1982) *J. Biol. Chem.* 257, 2049–2055.
55. Krebs, E. G. (1986) *Enzymes* (3rd Ed.) 17, 3–20.
56. Plowman, K. M., and Cleland, W. W. (1967) *J. Biol. Chem.* 242, 4239–4247.
57. Singh, M., Richards, E. G., Mukherjee, A., and Srere, P. A. (1976) *J. Biol. Chem.* 251, 5242–5250.
58. Hoffmann, G. E., Schiessl, J., and Weiss, L. (1979) *Hoppe-Seyler's Z. Physiol. Chem.* 360, 1445–1451.
59. Barnum, T. E. (1969) *Enzyme Handbook*, Springer-Verlag, New York.
60. Kurganov, B. I. (1982) *Allosteric Enzymes*, John Wiley & Sons, New York.
61. Ikeda, Y., Tanaka, T., and Noguchi, T. (1997) *J. Biol. Chem.* 272, 20495–20501.
62. Casazza, J. P., Veech, R. L. (1986) *Biochem. J.* 236, 635–641.
63. Klarlund, J. K., Bradfors, A. P., Milla, M. G., and Czech, M. P. (1990) *J. Biol. Chem.* 265, 227–234.
64. Alessi, D. R., Caudwell, F. B., Andjelkovic, M., Hemmings, B. A., and Cohen, P. (1996) *FEBS Lett.* 399, 333–338.
65. Sundqvist, K. E., Vuorinen, K. H., Peuhkurinen, K. J., and Hassinen, I. E. (1994) *Eur. Heart J.* 15, 561–570.
66. Barron, J. T., Kopp, S. J., Tow, J., and Parillo, J. E. (1994) *Am J. Physiol.* 267, H764–H769.
67. Comte, B., Vincent, G., Bouchard, B., Jette, M., Cordeau, S., and Rosiers, C. D. (1997) *J. Biol. Chem.* 272, 26125–26131.
68. Soboll, S., Scholz, R., Reisl, M., Elbers, R., and Heldt, H. W. (1976) in *Use of Isolated Liver Cells and Kidney Tubules in Metabolic Studies* (Tager, J. M., Soling, H. D., and Williamson, J. R., Eds.) pp 29–40, North-Holland Publishing Co., Amsterdam, The Netherlands.
69. Jamil, H., and Madsen, N. B. (1987) *J. Biol. Chem.* 262, 630–637.
70. Heinrich, R., and Schuster, S. (1996) in *Regulation of Cellular Systems*, Chapman and Hall, New York.

BI992159Y